

Supporting information

Mesopore-encaged active MnOx in nano-silica selectively suppressed lung cancer cell *via* induced autophagy effect

Fen Yang,^{†ac} Xuan Wang,^{†a} Jie Sun,^{†a} Sijia Tan,^{†a} Shizhe Zhou,^a Wenlong Tu,^b Xuexue Dong,^b Qikai Xiao,^a Fu Yang,^{*b} Liqian Gao,^{*a}

^aSchool of Pharmaceutical Sciences (Shenzhen), Sun Yat-sen University, Shenzhen 518107, P.R. China

^bSchool of Environmental and Chemical Engineering, Jiangsu University of Science and Technology, Zhenjiang 212003, Jiangsu, P. R. China

^cInstitute of Laboratory Medicine, Guangdong Provincial Key Laboratory of Medical Molecular Diagnostics, School of Medical Technology, The First Dongguan Affiliated Hospital, Guangdong Medical University, Dongguan, China

[†]These authors contributed equally.

Contents

1. Table S1. The IC ₅₀ value of these cell lines by induced MnO-MS.....	3
2. Figure S1. Wide-angle XRD pattern, survey spectrum, Mn2p Core level spectrum, DRUV-Vis spectrum, and FTIR spectrum of MnO-MS.....	3
3. Figure S2. The expression of LC3 protein level after treatment with MnO-MS.....	3
4. Figure S3. The data of Rh@MnO-MS.....	4
5. Figure S4. Data are presented as means ± SEM of Figure 4B.....	5
6. Figure S5. The reactive oxygen species (ROS) level of A549 cell by induced MnO-MS by flow cytometry.....	5
7. Figure S6. Mouse body weight of MnO-MS-treated A549 tumor-bearing nude mice and data of biochemical parameters.....	6

Table S1. The IC₅₀ value of these cell lines by induced MnO-MS.

Cell line	A549	HepG2	MCF-7	Huh7	U87	HeLa	THP1	HEK 293
IC ₅₀ (μg/mL)	11.19	11.50	11.54	18.57	67.42	132.5	>2000	>2000

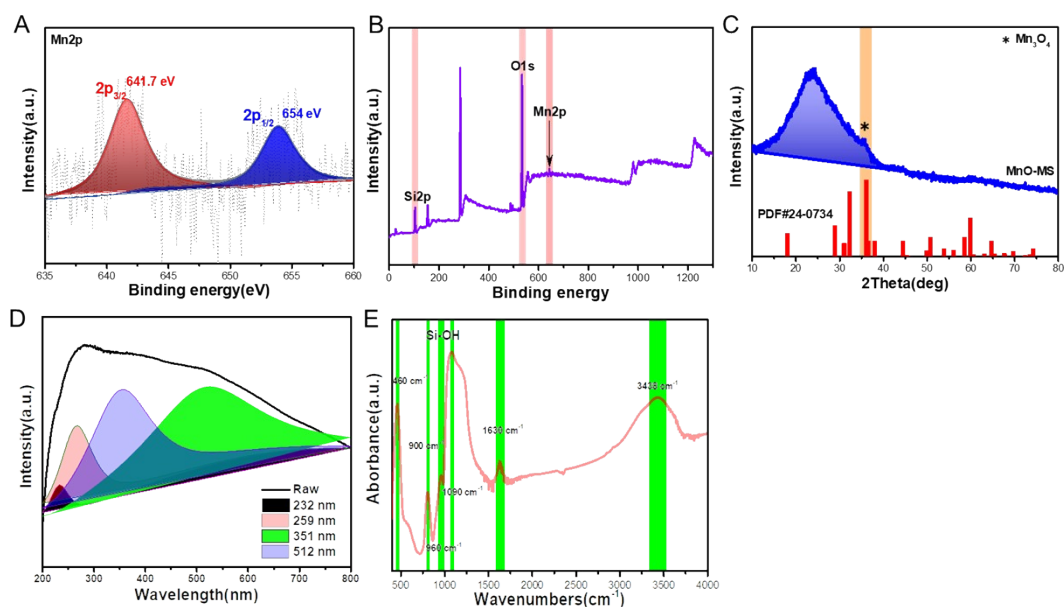


Figure S1. Wide-angle XRD pattern, survey spectrum, Mn2p Core level spectrum, DRUV-Vis spectrum, and FTIR spectrum of MnO-MS.

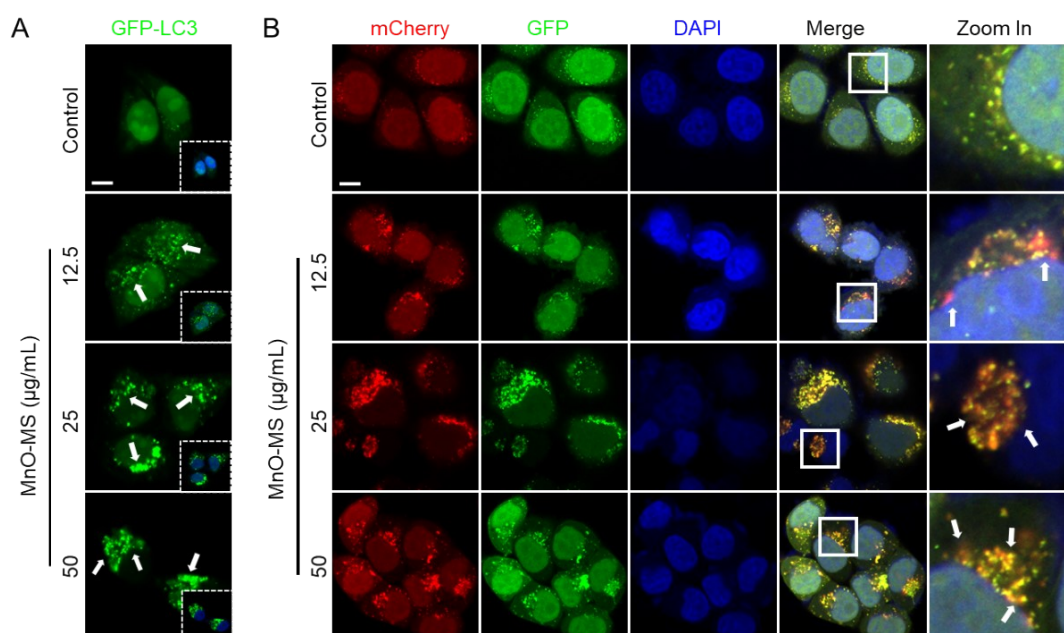


Figure S2. The expression of LC3 protein level after treatment with 12.5, 25, 50 μg/mL

MnO-MS in (A) GFP-LC3 HeLa cell or (B) mCherry-GFP-LC3 HeLa cell by laser scanning confocal microscope (LSCM). GFP is green, and mCherry is red and the nucleus was indicated with DAPI (blue). Scale bars: 10 μm . i) In the case of non-autophagy, mCherry-GFP-LC3 fusion protein exists in the cytoplasm by forming diffuse yellow fluorescence (the combined effect of mCherry (red) and GFP (green)); ii) In the case of autophagy, mCherry-GFP-LC3 fusion protein aggregated on the membrane of autophagosome and appeared yellow spots; iii) When autophagosome fused with the lysosome, it was shown as a red spot (mCherry) due to the partial quenching of GFP fluorescence.

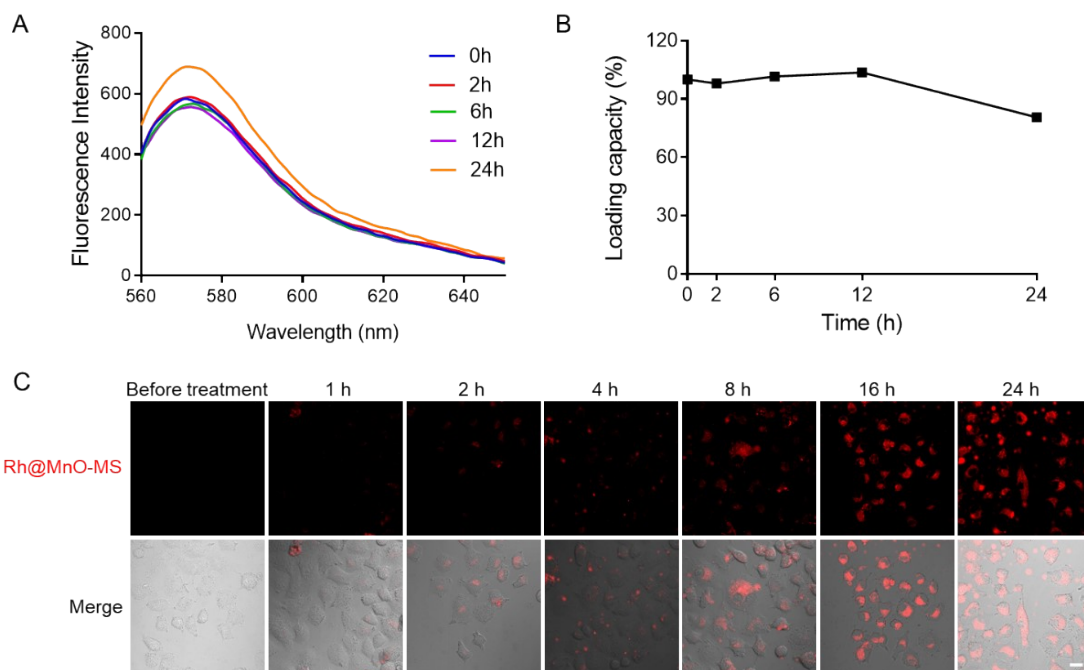


Figure S3. (A) The fluorescence intensity of Rh@MnO-MS in different time. (B) The loading capacity of Rh@MnO-MS in different time. (C) Fluorescence images of live A549 cells incubated with Rh@MnO-MS for 1, 2, 4, 8, 12, 24h. Red fluorescence shows location of the Rh@MnO-MS. Scale bars: 20 μm .

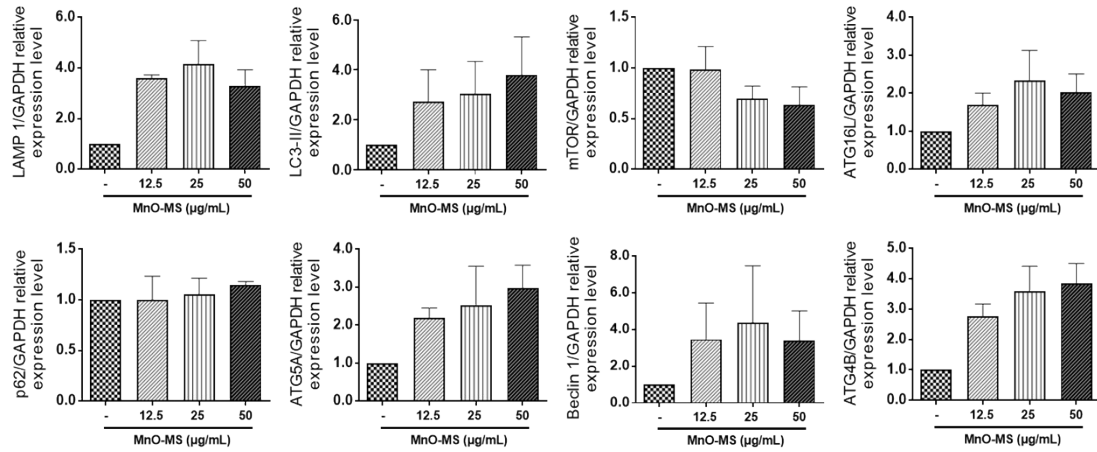


Figure S4. Data are presented as means ± SEM of **Figure 4B**.

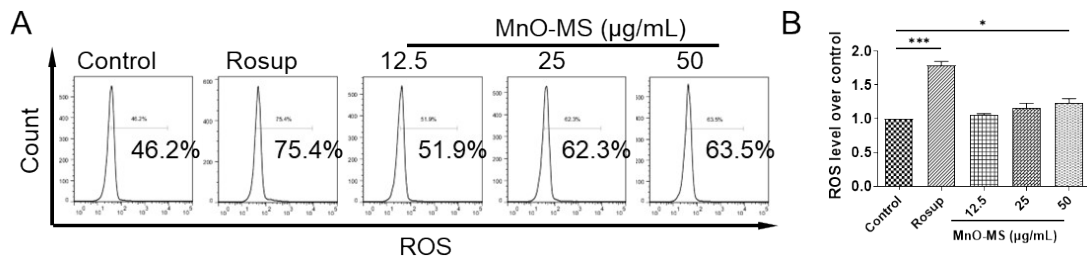


Figure S5. (A) The reactive oxygen species (ROS) level of A549 cell by induced MnO-MS (12.5, 25, 50 µg/mL) for 24h by flow cytometry, n=3 (B) Data are presented as means ± SEM. * $p < 0.05$, and *** $p < 0.001$ versus control group.

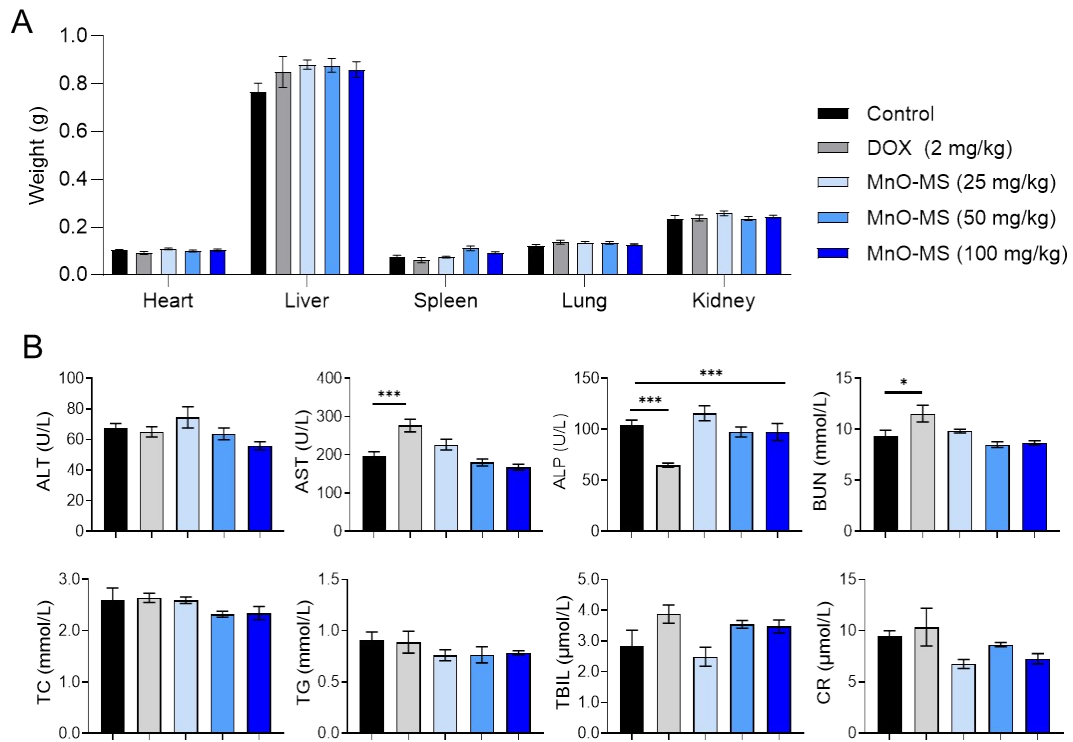


Figure S6. (A) Mouse body weight of MnO-MS-treated A549 tumor-bearing nude mice over 29 days. (B) Biochemical parameters including alanine aminotransferase (ALT), aspartate aminotransferase (AST), alkaline phosphatase (ALP), blood urea nitrogen (BUN), total cholesterol (TC), and triglyceride (TG), total bilirubin (TBIL) and creatinine (CR) of A549 tumor-bearing nude mice after 29-day of treatment. Data represent the mean \pm SEM (n=6). * $p < 0.05$, and *** $p < 0.001$ versus control group.